

## Optimization of $^{10}\text{Be}$ measurements at the 6 MV AMS facility DREAMS

Lachner, J.; Rugel, G.; Vivo Vilches, C.; Koll, D.; Stübner, K.; Winkler, S.; Wallner, A.;

Originally published:

February 2023

**Nuclear Instruments and Methods in Physics Research B 535(2023), 29-33**

DOI: <https://doi.org/10.1016/j.nimb.2022.11.008>

Perma-Link to Publication Repository of HZDR:

<https://www.hzdr.de/publications/Publ-34703>

Release of the secondary publication  
on the basis of the German Copyright Law § 38 Section 4.

CC BY-NC-ND

# Optimization of $^{10}\text{Be}$ measurements at the 6 MV AMS facility DREAMS

Johannes Lachner, Georg Rugel, Carlos Vivo-Vilches, Dominik Koll, Konstanze Stübner, Stephan Winkler, Anton Wallner

*Helmholtz-Zentrum Dresden-Rossendorf, Bautzner Landstr. 400, 01328 Dresden, Germany*

---

## Abstract

1 We investigated benefits from raising the ion beam energy during measurements of  $^{10}\text{Be}$  with Accelerator Mass  
2 Spectrometry (AMS) at the 6 MV DREAMS (DREsden AMS) facility. Increasing the terminal voltage to  $\geq 5$  MV  
3 hardly reduces the yield of the  $\text{Be}^{2+}$  charge state after the accelerator if one applies only a thin Ar gas stripper and  
4 makes use of an overpopulation of the 2+ charge state with respect to the expected equilibrium charge state yield. As  
5 a further stripping to the 4+ charge state is conducted in a degrader foil after the analysing magnet, it is desirable to hit  
6 the foil with the highest available velocity in order to have optimal stripping of  $\text{Be}^{2+}$  to the naked ion. The efficiency  
7 of  $^{10}\text{Be}$  measurements can be improved by ca. 36% if increasing the terminal voltage from 4.5 MV to 5.8 MV and  
8 already by 7.5% if going to 5.0 MV.

*Keywords:*  $^{10}\text{Be}$ , AMS, DREAMS, isobar suppression, beam transmission, beam energy

---

## 9 1. Introduction

10 Measurements of  $^{10}\text{Be}$  ( $T_{1/2}=1.39$  Myr, Korschinek et al. (2010); Chmeleff et al. (2010)) with DREAMS take up  
11 a large fraction of the AMS beam times at the 6 MV accelerator of the HZDR Ion Beam Center. This is a motivation  
12 to conduct these measurements under the most efficient conditions.  $^{10}\text{Be}$  detection potentially suffers from several  
13 interferences:  $^{10}\text{B}$  is the direct isobar and may cause secondary reactions, e.g. on protons in a silicon nitride foil  
14 producing the nuclear reaction  $^{10}\text{B}(p,\alpha)^7\text{Be}$  or via Rutherford scattering. Surviving  $^9\text{BeH}$  molecules are a potential  
15 interference if using a charge state lower than 3+ on the high energy side of the AMS system. However, all these  
16 interferences can be suppressed or avoided in modern AMS measurements, and blank levels of few  $10^{-15}$  and below  
17 have become the norm.

18 At larger systems ( $> 3$  MV terminal voltage) the more common setup is to use the 3+ charge state and a passive  
19 absorber stopping  $^{10}\text{B}^{3+}$ . The yield for the 3+ after the accelerator is a bit lower than the maximum value for the  
20 2+ using  $\text{O}_2$  (Hofmann et al., 1987) or Ar gas stripping (Niklaus et al., 1994). However, full isobar suppression and  
21 efficient  $^{10}\text{Be}$  detection can be achieved when directing the beam at this high energy of ca. 20 MeV directly onto a  
22 detector equipped with a passive absorber. This way, the overall transmission from the low-energy side of the system  
23 to events identified as  $^{10}\text{Be}$  in the detector can amount to 34% for a terminal voltage of 7.5 MV (Rood et al., 2013), to  
24 28% for 6 MV (Wilcken et al., 2017), and to 18% for a 5 MV facility (Maden et al., 2007; Xu et al., 2015). Highest  
25 efficiencies of overall 35% are reached at a terminal voltage of 7.8 MV by stripping the Be to the 3+ charge state and  
26 using a gas-filled magnet for detection (Wallner et al., 2022).

27 The common alternative in suppression of interferences is taking advantage of the element specific energy loss in a  
28 thin degrader foil (Raisbeck et al., 1984). At larger AMS facilities this is done with Ar stripping to the 2+ charge state  
29 followed by additional stripping in the foil, where the 4+ state presents the highest yield (Klein et al., 2008, 2011;  
30 Arnold et al., 2010; Akhmadaliev et al., 2013). The degrader foil technique has the advantage that a suitably designed  
31 AMS facility can be adapted in a rather simple way, i.e. by the insertion of the foil at the appropriate position, for a  
32  $^{10}\text{Be}$  measurement following previous measurements of other radioisotopes that do not require isobar suppression.

33 After major improvements in energy resolution for detection systems at low beam energies and using the thin and  
34 homogeneous silicon nitride foils as detector windows and for isobar suppression,  $^{10}\text{Be}$  measurements at compact  
35 (Müller et al., 2010) and intermediate AMS systems (Steier et al., 2019) have become more common in recent years.  
36 Initial efforts at compact AMS facilities to measure  $^{10}\text{Be}$  used the 2+ charge state (Grajcar et al., 2004). Then, rather  
37 than going for higher beam energy, the high yield of the 1+ charge state at terminal voltages  $<1$  MV was exploited  
38 (Müller et al., 2008). Still, the use of the 2+ charge state has also regained relevance for smaller AMS systems  
39 (Maxeiner et al., 2019; Seiler et al., 2018). For the most compact facilities this is motivated by its high yield at low  
40 velocities if stripping the Be with He gas (Lachner et al., 2014).

41 In the following we describe how the  $^{10}\text{Be}$  AMS measurement performance of the degrader foil technique can  
42 be significantly improved using terminal voltages between 5 and 6 MV. For this, we optimized the interplay between

43 acceleration voltage and Ar stripper gas pressure. We give the new performance numbers for DREAMS regarding  
 44  $^{10}\text{Be}$  determination.

## 45 2. Description of DREAMS for $^{10}\text{Be}$ measurements

46  $^{10}\text{Be}$  measurements are regularly undertaken at DREAMS since its installation (Akhmadaliev et al., 2013).  $\text{BeO}^-$   
 47 is extracted from solid  $\text{BeO}/\text{Nb}$  targets pressed into Cu cathodes using a Cs-sputter ion source type SO-110. Maximum  
 48 currents under routine measurement conditions can reach  $6\ \mu\text{A}$  in clean  $\text{BeO}$  material mixed in a weight ratio of  
 49  $\text{BeO}:\text{Nb}=1:4$  (Rugel et al., 2016). The beam is stripped in an Ar gas stripper on the high-voltage terminal of the 6 MV  
 50 tandemron (HVVE) accelerator and positive charge states are accelerated further. The measurement of  $^9\text{Be}^{2+}$  current is  
 51 conducted in an offset Faraday cup after a first mass-to-charge analysis in a  $90^\circ$  magnet.

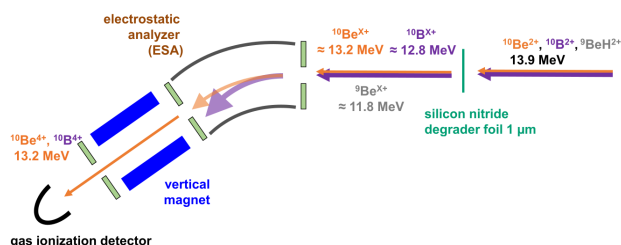


Figure 1: Schematic of the isobar separation using a silicon nitride degrader foil at DREAMS with exemplary numbers for a terminal voltage of 5.8 MV.

52 The  $2+$  beam with  $10\ \text{u}$  is directed onto the silicon nitride degrader foil (thickness  $1\ \mu\text{m}$ ,  $8\ \text{mm} \times 8\ \text{mm}$ ) (Fig. 1).  
 53 In this degrader foil any surviving molecular interference, e.g.  $^9\text{BeH}^{2+}$ , is broken up. Because of the high energy, the  
 54 majority of the  $^{10}\text{Be}$  ions is fully stripped in the foil. Therefore, ions in charge state  $4+$  are selected in the following  
 55  $35^\circ$  ESA and the  $30^\circ$  vertical magnet. The different energy loss is utilized to separate the major part of the  $^{10}\text{B}$   
 56 interference out of the beam.

57 The  $^{10}\text{Be}^{4+}$  beam is directed into the gas ionization chamber (silicon nitride entrance foil: thickness  $75\ \text{nm}$ ,  
 58  $8\ \text{mm} \times 8\ \text{mm}$ ) that is filled with isobutane (pressure range for our experiments:  $25\ \text{mbar}$ - $37\ \text{mbar}$ ). Signals from  
 59 the four separate anodes can be used to distinguish the incoming ions and to separate the  $^{10}\text{Be}$  from  $^{10}\text{B}$  with the same  
 60 energy, from scattered  $^{10}\text{B}$ , from  $^9\text{Be}$  fragments of a  $^9\text{BeH}$  molecule breakup, and from rare  $m/q$  interferences such  
 61 as  $^{15}\text{N}^{6+}$ . The slits in the system generally can be kept open during the measurement. Thus, the possible locations  
 62 for ion beam losses due to geometric limitations are the stripper canal, the degrader foil and the entrance foil to the  
 63 detector. Normalization is conducted using the reference material SMD-Be-12 with a nominal  $^{10}\text{Be}/^9\text{Be}$  ratio of  $1.704$   
 64  $\pm 0.030$  ·  $10^{-12}$  (Akhmadaliev et al., 2013).

### 3. Transmission through the accelerator

Previous systematic work on the charge state yield of Be from  $\text{BeO}^-$  in gas and foil strippers was performed at the 6 MV tandem accelerator in Zurich in their efforts to determine measurement conditions for  $^{10}\text{Be}$  (Hofmann et al., 1987; Niklaus et al., 1994). From their measurements they give an optimal value for  $^{10}\text{Be}$  transmission from  $\text{BeO}^-$  injection into the accelerator at 4.5 MV under equilibrium charge state conditions. The equilibrium of charge states is reached if small changes of the stripper gas density do not change the yield of the individual charge states anymore. Typically, below the target thickness necessary to reach charge state equilibrium, the so-called non-equilibrium case, the population of 1+ and 2+ is increased relative to the equilibrium value at the respective energy. Similarly, it was observed for a series of heavier ions that at MeV energies a thin stripper is already sufficient to populate charge states  $>1+$  (Hotchkis et al., 2013). This effect of overpopulation of a charge state at low stripper pressures can be exploited if no suppression of molecular background in the stripping process is required.

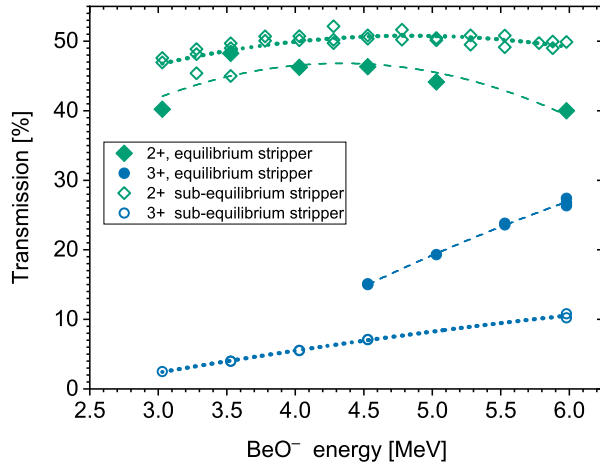


Figure 2: Transmission data for a Be beam from  $\text{BeO}^-$  in Ar gas measured at DREAMS.

In our experiments at the DREAMS facility we focused on an optimization of the AMS method. Thus, we only give the raw beam transmission data (Fig. 2) for the  $^9\text{Be}$  beam from  $^9\text{Be}^{16}\text{O}^-$  breakup. We did not perform scans of the stripper pressure at each voltage setting, which would be necessary to deduce the equilibrium charge state yield at each terminal voltage. We find the maximum stripping yield for the 2+ charge state at a terminal voltage  $\approx 4.5$  MV. However, the decrease of transmission if increasing the energy is little: at the maximum terminal voltage of 6 MV the transmission is 50% and thus only 2 percentage points less than the maximum value.

In comparison to  $^9\text{Be}$ , the  $^{10}\text{Be}$  from the breakup of  $^{10}\text{Be}^{16}\text{O}^-$  has a lower velocity by the factor of  $\sqrt{25/26}$  in the stripper channel at a given acceleration voltage. The respective maximum for the charge state yield of  $^{10}\text{Be}^{2+}$  is shifted relative to the data shown for  $^{10}\text{Be}^{2+}$  in Fig. 2 and is rather at  $\approx 4.7$  MV.

#### 4. Energy loss measurements in the silicon nitride degrader foil

From the point of optimizing counting statistics it already becomes clear that an increase of the terminal voltage from 4.5 MV to 4.7 MV can improve the transport of  $^{10}\text{Be}^{2+}$  to the high-energy side of the system. In addition, one has to consider the energy loss and the second stripping process in the degrader foil. In the study of Nottoli et al. (2013) at the ASTER facility it is shown that the energy loss of  $^{10}\text{Be}$  and  $^{10}\text{B}$  at a beam energy of 10.7 MeV (corresponding to a terminal voltage of 4.5 MV) in the degrader foil is described well by several theoretical models with slightly better agreement between theoretical estimations and experimental values for Be than for B.

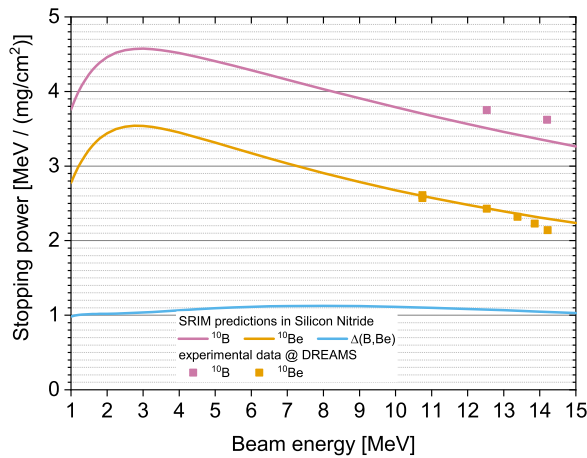


Figure 3: Comparison of experimental stopping powers in the  $1\ \mu\text{m}$  degrader foil for  $^{10}\text{Be}$  and  $^{10}\text{B}$  beams with estimated energy loss from SRIM (Ziegler et al., 2013).

Here, we present an extension of experimental data (Fig. 3), and compare it to data estimated with SRIM, the most commonly used model for energy loss estimations (Ziegler et al., 2013). Same as Nottoli et al. (2013), we used our  $35^\circ$  ESA (Radius 2.6 m, plate distance 3.6 cm) to measure the energy of the beam after the foil. In all tests, lenses and the vertical  $30^\circ$  magnet were also tuned for optimal transmission to the detector. Subtracting the energy measured with the  $35^\circ$  ESA after the foil from the energy estimated from the acceleration given by the terminal voltage gives the experimental energy loss. This energy loss is converted to a mean stopping power  $dE/dx$  in  $\text{MeV}/(\text{mg}/\text{cm}^2)$  by using a density of the silicon nitride foil of  $3.1\ \text{g}/\text{cm}^3$  (Sun et al., 2007). For the model calculations a composition of  $\text{Si}_3\text{N}_{3.1}$  was assumed.

The experimentally determined energy loss for Be fits well with the predictions of SRIM, while the experimental values for B are higher (Fig. 3). This confirms the previous measurements by Nottoli et al. (2013). The separation of  $^{10}\text{Be}$  and  $^{10}\text{B}$  via their energy loss in the silicon nitride foil at beam energies between 10 and 15 MeV is thus about 20% better than predicted by the model.

104 **5. Detection efficiency for  $^{10}\text{Be}$**

105 For the measurements at the different final beam energies we thoroughly tuned all the beam transport parameters  
 106 on the high-energy side of the system. In addition, the gas pressure in the ionization detector was adapted such that  
 107 the  $^{10}\text{Be}$  ions deposit a similar energy on the final of the four anodes. All other major interferences are stopped on the  
 108 third anode at the latest. This way, suppression of all the interferences remains unchanged for all energies tested. As  
 109 an example, Fig. 4 shows a spectrum of the reference material SMD-Be-12 recorded at a final energy of 13.86 MeV. In  
 110 tests of other materials, including samples prepared by various users, only the relative intensities of the other species  
 111 ( $^9\text{Be}$ ,  $^{10}\text{B}$ ,  $^{15}\text{N}$ ) varied, and no additional ion species was visible in the spectra.

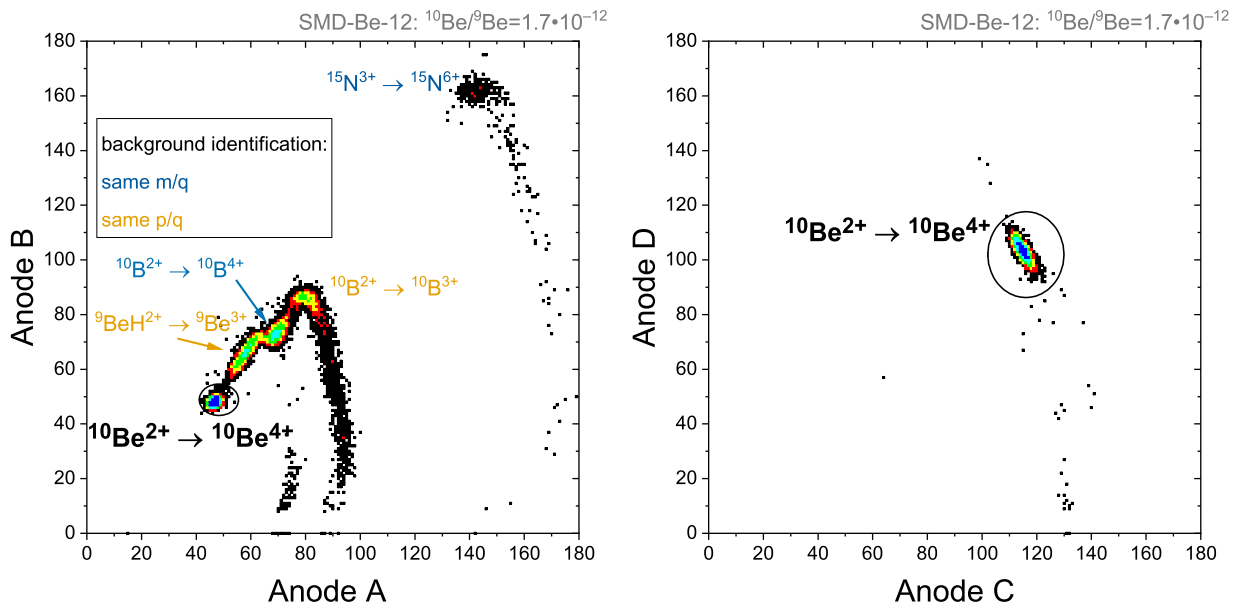


Figure 4: Spectra of reference material SMD-Be-12 in the gas ionization detector at a  $^{10}\text{Be}$  total energy of 13.86 MeV (terminal voltage of 5.81 MV).

112 Increasing the energy of the 10 u beam entering the foil we observe the expected increase in the measured  $^{10}\text{Be}/^9\text{Be}$   
 113 ratio relative to the sample ratio due to the increasing yield of the 4+ charge state (Fig. 5). At 5.8 MV some of the  
 114 lenses are close to their maximum power, so it seems that optical transmission of the system is reaching its limits at  
 115 this terminal voltage for  $\text{Be}^{2+}$  from  $\text{BeO}^-$ . For an increase of the terminal voltage  $>5.9$  MV we do not reach a further  
 116 gain in the correction factor. As such an increase already comes with small losses in the  $\text{Be}^{2+}$  stripping transmission  
 117 (Fig. 2), the optimal setting at DREAMS is at a terminal voltage of 5.8 MV.

118 The maximum possible transmission through the foil is given by the equilibrium 4+ charge state yield of  $^{10}\text{Be}$   
 119 when being stripped. Experimental values are available for stripping Be in a carbon foil (Shima et al., 1989) and  
 120 suggest a 4+ yield of close to 80% after the foil at a  $^{10}\text{Be}$  energy of ca. 13 MeV. In comparison to this, the DREAMS  
 121 experimental values are still low. Either this reflects losses between the foil and the detector or a lower yield for the  
 122 4+ in the  $1\ \mu\text{m}$  silicon nitride foil.

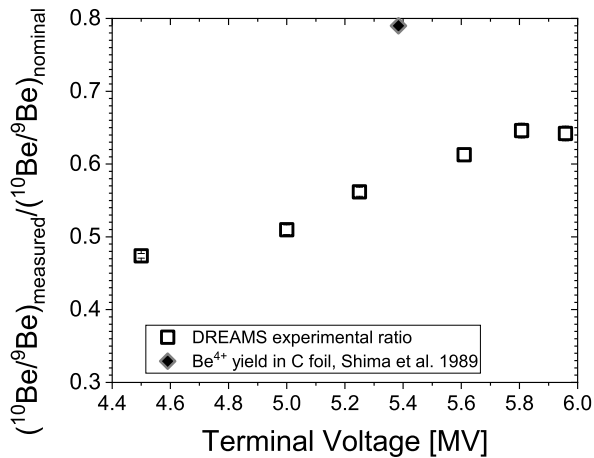


Figure 5: Measured to nominal  $^{10}\text{Be}/^9\text{Be}$  ratios of reference material SMD-Be-12 relative to the terminal voltage at which the measurement was conducted. As measurements of  $^9\text{Be}$  and  $^{10}\text{Be}$  are conducted on the high-energy side of the system, this does not reflect changes in transmission through the accelerator. For comparison the equilibrium charge state yield of  $^{10}\text{Be}^{4+}$  in a carbon foil according to Shima et al. (1989) is also presented.

123 The  $^{10}\text{Be}^{4+}/^9\text{Be}^{2+}$  ratio of the standards is measured at ca. 65% of the nominal value if the accelerator is set to  
 124 5.8 MV. The correction factor thus is reduced from previously 2.2 at 4.5 MV (Akhmadaliev et al., 2013) to 1.5. Under  
 125 these conditions the transport efficiency from the low energy side to the detector is 32.5%. Similarly, an increase of  
 126 the terminal voltage to 5.0 MV leaves the transmission at 50% and already reduces the correction factor to 2.0, thus  
 127 reaching an overall transport efficiency from the low energy side to the detector of 25%. The absolute difference in  
 128 energy loss between  $^{10}\text{Be}$  and  $^{10}\text{B}$  does not change with higher energy. Thus, there is no strong negative effect of the  
 129 beam energy increase on the separation of isobars by the degrader foil. Moreover, the higher energy of the ions leads  
 130 to a better resolution in terms of signal height vs. signal width improving the separation of other interferences. This  
 131 way, the low-level carrier material Phena EA (Merchel et al., 2013) can still be measured at levels of ca.  $2 \cdot 10^{-16}$  at  
 132 increased beam energies.

## 133 6. Conclusion

134 Using a reduced Ar gas stripper density the  $^{10}\text{Be}$  measurements can be conducted at higher terminal voltages in a  
 135 non-equilibrium charge exchange conditions without losing too much beam intensity. This leads to higher available  
 136 beam energies for the extracted  $^{10}\text{Be}^{2+}$  beam in the isobar suppression on the degrader foil. The higher efficiency  
 137 for counting  $^{10}\text{Be}$  events will save time or improve the counting statistics for the  $^{10}\text{Be}$  measurement. Yet it has to be  
 138 considered that operation of the tandem accelerator close to its maximum voltage may require additional time due to  
 139 previous conditioning of the high voltage.

140 The optimal conditions for  $^{10}\text{Be}$  measurements at the 6 MV DREAMS facility are reached by running the system  
 141 at a terminal voltage of 5.8 MV and thus transporting 32.5% of the  $^{10}\text{Be}$  from the low energy side to the detector.  
 142 Potentially, the use of a larger sized or thinner foil at the degrader and a larger detector window could increase the



143 acceptance of the system and thus further improve this value. However, this would come at a decrease in separation of  
144 other interferences. Presently, interferences from the isobar  $^{10}\text{B}^{4+}$ , molecular breakup fragment  $^9\text{Be}^{3+}$  from  $^9\text{BeH}^{2+}$ ,  
145 equal m/q species  $^{15}\text{N}^{6+}$  or from scattered  $^{10}\text{B}^{3+}$  are clearly separated, and count rates are well manageable with the  
146 gas ionization detector.  $^{10}\text{Be}/^9\text{Be}$  levels of  $2 \cdot 10^{-16}$  are reached with suitable Be blank materials.

## 147 Acknowledgements

148 This research was carried out at the Ion Beam Centre (IBC) at the Helmholtz-Zentrum Dresden-Rossendorf e.V.,  
149 a member of the Helmholtz Association. We would like to thank the DREAMS operator team for their assistance with  
150 AMS measurements. Special thanks go to Silke Merchel, Toralf Döring, Sebastian Fichter, René Ziegenrucker and  
151 Sebastian Zwickel for discussions and assistance during the experiments.

## 152 References

- 153 G. Korschinek, A. Bergmaier, T. Faestermann, U. Gerstmann, K. Knie, G. Rugel, A. Wallner, I. Dillmann, G. Dollinger, C. L. von Gostomski,  
154 K. Kossert, M. Maiti, M. Poutivtsev, A. Remmert, A new value for the half-life of  $^{10}\text{Be}$  by Heavy-Ion Elastic Recoil Detection and liquid  
155 scintillation counting, *Nucl. Instrum. Meth. B* 268 (2010) 187–191.
- 156 J. Chmeleff, F. von Blanckenburg, K. Kossert, D. Jakob, Determination of the  $^{10}\text{Be}$  half-life by multicollector ICP-MS and liquid scintillation  
157 counting, *Nucl. Instrum. Meth. B* 268 (2010) 192–199.
- 158 H. Hofmann, G. Bonani, M. Suter, W. Wölfli, Charge state distributions and isotopic fractionation, *Nucl. Instrum. Meth. B* 29 (1987) 100–104.  
159 doi:[https://doi.org/10.1016/0168-583X\(87\)90214-X](https://doi.org/10.1016/0168-583X(87)90214-X).
- 160 T. Niklaus, G. Bonani, Z. Guo, M. Suter, H.-A. Synal, Optimising tandem accelerator stripping efficiency by simulation of charge changing  
161 processes, *Nucl. Instrum. Meth. B* 92 (1994) 115–121. doi:[https://doi.org/10.1016/0168-583X\(94\)95989-7](https://doi.org/10.1016/0168-583X(94)95989-7).
- 162 D. H. Rood, T. A. Brown, R. C. Finkel, T. P. Guilderson, Poisson and non-Poisson uncertainty estimations of  $^{10}\text{Be}/^9\text{Be}$  measurements at  
163 LLNL-CAMS, *Nucl. Instrum. Meth. B* 294 (2013) 426–429. doi:<https://doi.org/10.1016/j.nimb.2012.08.039>.
- 164 K. Wilcken, D. Fink, M. Hotchkis, D. Garton, D. Button, M. Mann, R. Kitchen, T. Hauser, A. O'Connor, Accelerator Mass Spectrometry on  
165 SIRIUS: New 6 MV spectrometer at ANSTO, *Nucl. Instrum. Meth. B* 406 (2017) 278–282. doi:[https://doi.org/10.1016/j.nimb.2017.](https://doi.org/10.1016/j.nimb.2017.01.003)  
166 01.003.
- 167 C. Maden, P. Anastasi, A. Dougans, S. Freeman, R. Kitchen, G. Klody, C. Schnabel, M. Sundquist, K. Vanner, S. Xu, SUERC AMS ion detection,  
168 *Nucl. Instrum. Meth. B* 259 (2007) 131–139. doi:<https://doi.org/10.1016/j.nimb.2007.01.151>.
- 169 S. Xu, S. P. Freeman, D. H. Rood, R. P. Shanks, Decadal  $^{10}\text{Be}$ ,  $^{26}\text{Al}$  and  $^{36}\text{Cl}$  QA measurements on the SUERC 5 MV accelerator mass spectrometer,  
170 *Nucl. Instrum. Meth. B* 361 (2015) 39–42. doi:<https://doi.org/10.1016/j.nimb.2015.03.064>.
- 171 A. Wallner, L. Fifield, M. Froehlich, D. Koll, G. Leckenby, M. Martschini, S. Pavetich, S. Tims, D. Schumann, Z. Slavkovská, AMS with a 14  
172 million volt accelerator - Mn-53 and Fe-60 with ANU's ENGE, *Nucl. Instrum. Meth. B* this proceedings (2022).
- 173 G. Raisbeck, F. Yiou, D. Bourles, J. Lestringuez, D. Deboffe, Measurement of  $^{10}\text{Be}$  with a tandem accelerator operating at 2 MV, *Nucl. Instrum.*  
174 *Meth. B* 5 (1984) 175–178.
- 175 M. Klein, A. Gott dang, D. Mous, D. Bourlès, M. Arnold, B. Hamelin, G. Aumaître, R. Braucher, S. Merchel, F. Chauvet, Performance of  
176 the HVE 5 MV AMS system at CEREGE using an absorber foil for isobar suppression, *Nucl. Instrum. Meth. B* 266 (2008) 1828–1832.  
177 doi:<https://doi.org/10.1016/j.nimb.2007.11.077>.
- 178 M. Klein, A. Dewald, A. Gott dang, S. Heinze, D. Mous, A new HVE 6 MV AMS system at the University of Cologne, *Nucl. Instrum. Meth. B*  
179 269 (2011) 3167–3170. doi:<https://doi.org/10.1016/j.nimb.2011.04.024>.

180 M. Arnold, S. Merchel, D. L. Bourlès, R. Braucher, L. Benedetti, R. C. Finkel, G. Aumaître, A. Gott dang, M. Klein, The French accelerator  
181 mass spectrometry facility ASTER: Improved performance and developments, *Nucl. Instrum. Meth. B* 268 (2010) 1954–1959. doi:https:  
182 //doi.org/10.1016/j.nimb.2010.02.107.

183 S. Akhmadaliev, R. Heller, D. Hanf, G. Rugel, S. Merchel, The new 6 MV AMS-facility DREAMS at Dresden, *Nucl. Instrum. Meth. B* 294 (2013)  
184 5–10. doi:https://doi.org/10.1016/j.nimb.2012.01.053.

185 A. Müller, M. Christl, J. Lachner, M. Suter, H.-A. Synal, Competitive  $^{10}\text{Be}$  measurements below 1MeV with the upgraded ETH-TANDY AMS  
186 facility, *Nucl. Instrum. Meth. B* 268 (2010) 2801–2807. doi:https://doi.org/10.1016/j.nimb.2010.05.104.

187 P. Steier, M. Martschini, J. Buchriegler, J. Feige, J. Lachner, S. Merchel, L. Michlmayr, A. Priller, G. Rugel, E. Schmidt, A. Wallner, E. M. Wild,  
188 R. Golser, Comparison of methods for the detection of  $^{10}\text{Be}$  with AMS and a new approach based on a silicon nitride foil stack, *Int. J. Mass*  
189 *Spectrom.* 444 (2019) 116175.

190 M. Grajcar, M. Döbeli, P. Kubik, C. Maden, M. Suter, H.-A. Synal,  $^{10}\text{Be}$  measurements with terminal voltages below 1 MV, *Nucl. Instrum. Meth.*  
191 *B* 223-224 (2004) 190–194.

192 A. Müller, M. Christl, M. Döbeli, P. Kubik, M. Suter, H.-A. Synal,  $^{10}\text{Be}$  AMS measurements at low energies ( $E < 1\text{MeV}$ ), *Nucl. Instrum. Meth. B*  
193 266 (2008) 2207–2212. doi:https://doi.org/10.1016/j.nimb.2008.02.067.

194 S. Maxeiner, H.-A. Synal, M. Christl, M. Suter, A. Müller, C. Vockenhuber, Proof-of-principle of a compact 300 kV multi-isotope AMS facility,  
195 *Nucl. Instrum. Meth. B* 439 (2019) 84–89. doi:https://doi.org/10.1016/j.nimb.2018.11.028.

196 M. Seiler, J. Anjar, E. Vaernes, M.-J. Nadeau, G. Scognamiglio, First  $^{10}\text{Be}$  measurements at Trondheim 1 MV AMS, *Nucl. Instrum. Meth. B* 437  
197 (2018) 123–129. doi:https://doi.org/10.1016/j.nimb.2018.08.013.

198 J. Lachner, M. Christl, A. M. Müller, M. Suter, H.-A. Synal,  $^{10}\text{Be}$  and  $^{26}\text{Al}$  low-energy AMS using He-stripping and background suppression via  
199 an absorber, *Nucl. Instrum. Meth. B* 331 (2014) 209–214. doi:https://doi.org/10.1016/j.nimb.2013.11.034.

200 G. Rugel, S. Pavetich, S. Akhmadaliev, S. M. Enamorado Baez, A. Scharf, R. Ziegenrucker, S. Merchel, The first four years of the AMS-  
201 facility DREAMS: Status and developments for more accurate radionuclide data, *Nucl. Instrum. Meth. B* 370 (2016) 94–100. doi:https:  
202 //doi.org/10.1016/j.nimb.2016.01.012.

203 M. Hotchkis, D. Child, D. Fink, V. Levchenko, A. Wallner, Investigation of gas stripping at 4.1MeV for high mass negative ions, *Nucl. Instrum.*  
204 *Meth. B* 294 (2013) 387–391. doi:https://doi.org/10.1016/j.nimb.2012.01.019.

205 E. Nottoli, M. Arnold, G. Aumaître, D. L. Bourlès, K. Keddadouche, M. Suter, The physics behind the isobar separation of  $^{36}\text{Cl}$  and  $^{10}\text{Be}$  at the  
206 French AMS national facility ASTER, *Nucl. Instrum. Meth. B* 294 (2013) 397 – 402.

207 J. Ziegler, J. Biersack, M. Ziegler, SRIM - The Stopping and Range of Ions in Matter, 2013. [Http://www.srim.org](http://www.srim.org).

208 G. Sun, M. Döbeli, A. Müller, M. Stocker, M. Suter, L. Wacker, Energy loss and straggling of heavy ions in silicon nitride in the low MeV energy  
209 range, *Nucl. Instrum. Meth. B* 256 (2007) 586–590.

210 K. Shima, N. Kuno, M. Yamanouchi, Systematics of equilibrium charge distributions of ions passing through a carbon foil over the ranges  $Z=4-92$   
211 and  $E=0.02-6\text{ MeV/u}$ , *Phys. Rev. A* 40 (1989) 3557–3570. doi:10.1103/PhysRevA.40.3557.

212 S. Merchel, W. Bremser, D. L. Bourlès, U. Czeslik, J. Erzinger, N.-A. Kummer, L. Leanni, B. Merkel, S. Recknagel, U. Schaefer, Accu-  
213 racy of  $^9\text{Be}$ -data and its influence on  $^{10}\text{Be}$  cosmogenic nuclide data, *J. Radioanal. Nucl. Chem.* 298 (2013) 1871–1878. doi:10.1007/  
214 s10967-013-2746-x.